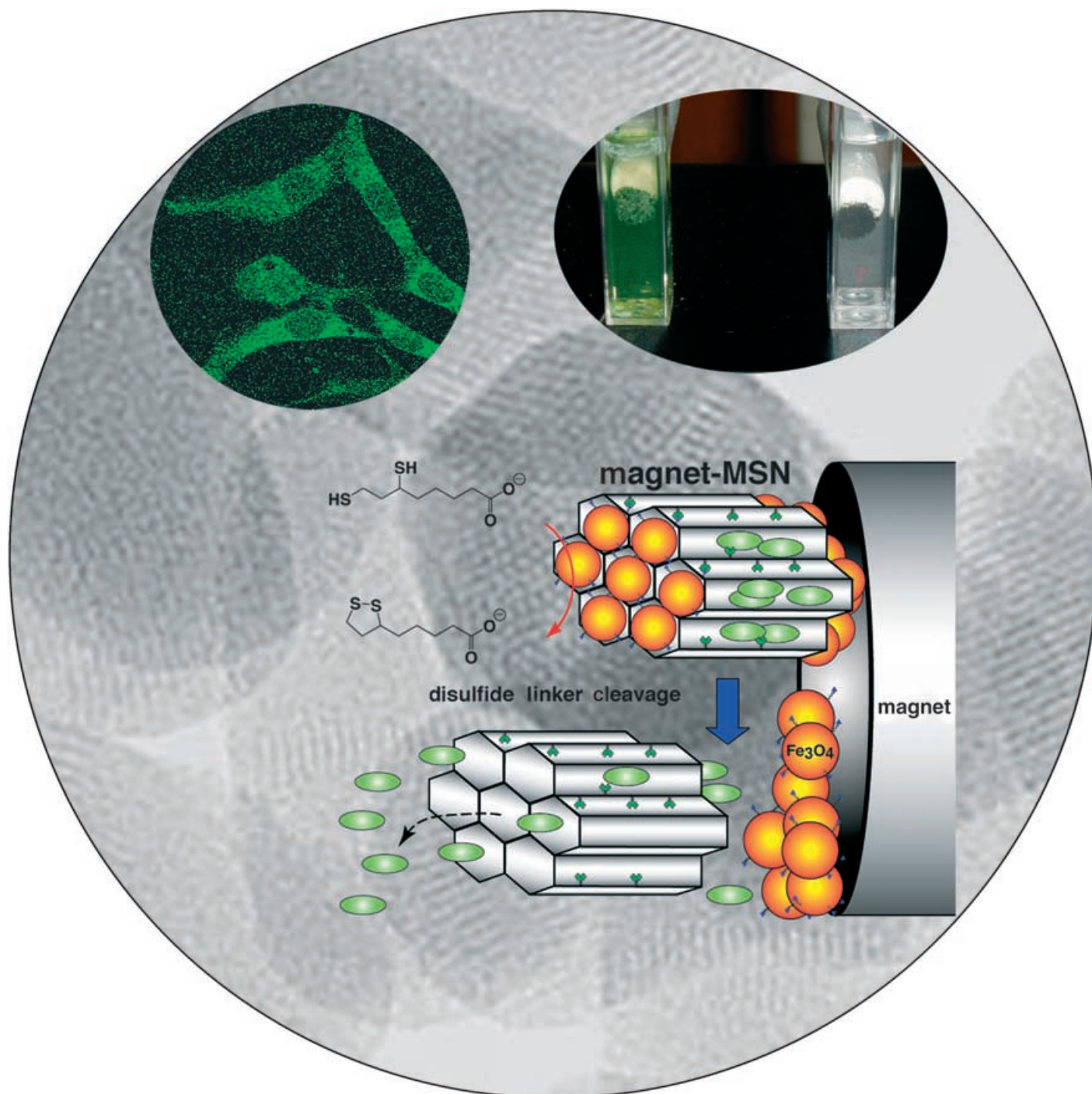


Communications



The controlled release of fluorescein from a mesoporous silica/superparamagnetic iron oxide core/shell nanodevice in the presence of an external magnetic field takes place by using cell-produced antioxidants as stimuli. For more information on this promising approach to drug-delivery systems, see the Communication by V. S.-Y. Lin and co-workers on the following pages.

Stimuli-Responsive Controlled-Release Delivery System Based on Mesoporous Silica Nanorods Capped with Magnetic Nanoparticles**

Supratim Giri, Brian G. Trewyn, Michael P. Stellmaker, and Victor S.-Y. Lin*

Recent reports on surface-functionalized, superparamagnetic iron oxide nanoparticles have demonstrated their feasibility for use in a variety of biological applications such as drug/gene delivery,^[1–5] magnetic resonance imaging,^[6–9] bioseparation,^[10–13] tissue repairing,^[14] and thermal tumor therapy.^[15–18] In contrast, only a few examples of controlled-release drug-delivery systems based on magnetic nanoparticles have been reported.^[19,20] Most of these systems comprise magnetic nanoparticle “cores” coated with organic or inorganic “shell” constituents, and encapsulated within the layers of shells are the pharmaceutical drugs. In the presence of an external magnetic field, these core-shell materials are attracted toward the magnet. This magnetic motor effect is indeed attractive for the development of site-specific drug-delivery systems. However, many important site-selective delivery systems, such as those for highly toxic antitumor drugs, require “zero release” before reaching the targeted cells or tissues. To the best of our knowledge, no controlled-release delivery systems based on magnetic nanoparticles that are stimuli-responsive and capable of “zero premature release” have been reported.

Surface-functionalized mesoporous silica materials have been demonstrated to be excellent hosts of molecules of various sizes, shapes, and functionalities.^[21–28] Recent reports^[29–33] on the design of capped and gated mesoporous silica derivatives have shown promise in the generation of controlled-release nanodevices. Herein, we report the synthesis of a controlled-release delivery system that is based on MCM-41-type mesoporous silica nanorods (MSNs) capped with superparamagnetic iron oxide nanoparticles and is stimuli-responsive and chemically inert to guest molecules entrapped in the matrix.

The system consists of MSNs functionalized with 3-(propyldisulfanyl)propionic acid to give “linker-MSNs”, which have an average particle size of 200 nm × 80 nm (length × width) and an average pore diameter of around

3.0 nm. As a proof of principle, fluorescein was used as the guest molecule to be encapsulated inside the linker-MSN material. By introducing dry linker-MSNs to an aqueous solution of fluorescein, the mesopores of the MSNs behaved like sponges by soaking up fluorescein molecules (Figure 1). Next, the openings of the mesopores of the fluorescein-loaded linker-MSN were covalently capped in situ through amidation^[34] of the 3-(propyldisulfanyl)propionic acid functional groups bound at the pore surface with 3-aminopropyltriethoxysilyl-functionalized superparamagnetic iron oxide (APTS-Fe₃O₄) nanoparticles.^[35] The disulfide linkages between the MSNs and the Fe₃O₄ nanoparticles are chemically labile and can be cleaved with various cell-produced antioxidants and disulfide reducing agents such as dihydro-lipoic acid (DHLA) and dithiothreitol (DTT), respectively. The release of the magnetic nanoparticle caps from the fluorescein-loaded MSNs can be regulated by the concentration of trigger molecules (Figure 1).

The mercaptopropyl-derivatized mesoporous silica nanorods (thiol-MSNs) were initially prepared according to our previously reported co-condensation method.^[31,33,36–41] After removal of the surfactant, thiol-MSNs were treated with 2-carboxyethyl-2-pyridyl disulfide to yield the acid-functionalized linker-MSNs. The rod shape, the average particle size, and the MCM-41-type mesoporous structure of the linker-MSNs were confirmed by transmission electron microscopy (TEM). The mesopores (porous channels) are represented by the alternating black and white stripes as shown in Figure 2a. The N₂ sorption isotherms of the material further revealed a BET isotherm typical of an MCM-41 structure (type IV), with a surface area of 1018.0 m² g^{−1} and a narrow BJH pore-size distribution (average pore diameter: 3.0 nm).^[42]

The superparamagnetic Fe₃O₄ nanoparticles coated with 3-aminopropylsiloxy groups (APTS-Fe₃O₄) were prepared according to a reported procedure.^[34] The TEM micrograph (Figure 2b) of the resultant APTS-Fe₃O₄ particles revealed an average diameter of 10 nm for the particles. APTS-Fe₃O₄ nanoparticles (960.00 mg) were treated with the linker-MSNs (80.00 mg) in a solution of fluorescein (3.60 μM) in PBS medium (100.0 mM, pH 7.4). The resulting suspensions were centrifuged, and the Fe₃O₄-MSN-fluorescein material (magnet-MSNs) along with the unreacted APTS-Fe₃O₄ nanoparticles were isolated by filtration. The concentration of fluorescein in the filtrate was determined by UV/Vis spectroscopy to be 1.50 μM. The decrease in the concentration of fluorescein in solution (≈ 2.10 μM) was attributed to the uptake of 1.68 × 10^{−8} moles of fluorescein by the MSNs which corresponds to a loading efficiency of approximately 58.3 mol %.

The successful incorporation of APTS-Fe₃O₄ nanoparticles in the MSN matrix was confirmed by various spectroscopic methods. The covalent immobilization of the surface-functionalized Fe₃O₄ nanoparticles to the linker-MSN led to a decrease in intensity of the powder X-ray diffraction (XRD) peaks (Figure 3a). Such a decrease in scattering contrast between the pores and the framework of the MCM-41 materials as a result of pore-filling has been reported previously.^[43–46] Furthermore, a small increase was observed in the *d*₁₀₀ (spacing) value of the Fe₃O₄-capped magnet-MSNs

[*] S. Giri, B. G. Trewyn, M. P. Stellmaker, Prof. Dr. V. S.-Y. Lin
Department of Chemistry and U.S. DOE Ames Laboratory
Iowa State University
Ames, Iowa 50011 (USA)
Fax: (+1) 515-294-0105
E-mail: vsylin@iastate.edu

[**] We thank the U.S. National Science Foundation (grant nos. CHE-0239570 and CMS-0409625) for financial support of this research.

Supporting information for this article is available on the WWW under <http://www.angewandte.org> or from the author.

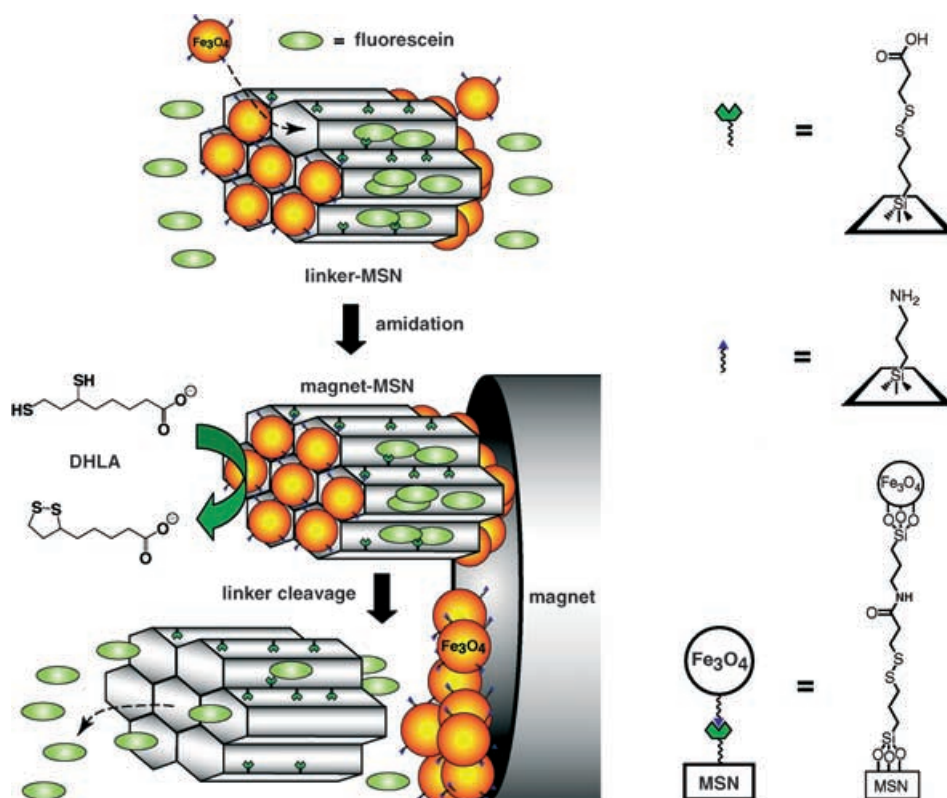


Figure 1. Schematic of the stimuli-responsive delivery system (magnet-MSN) based on mesoporous silica nanorods capped with superparamagnetic iron oxide nanoparticles. The controlled-release mechanism of the system is based on reduction of the disulfide linkage between the Fe_3O_4 nanoparticle caps and the linker-MSN hosts by reducing agents such as DHLA.

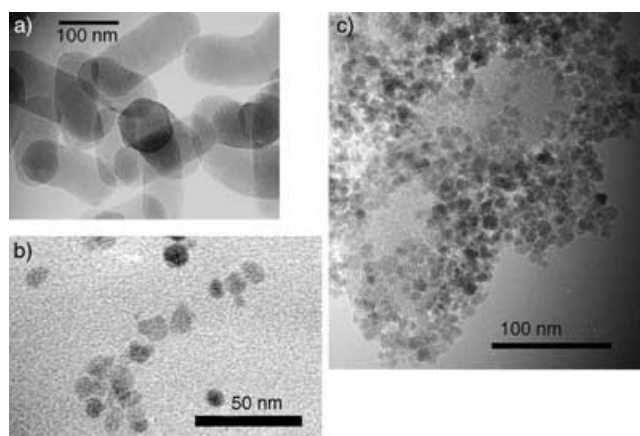


Figure 2. TEM images of a) linker-MSNs, b) APTS-coated Fe_3O_4 nanoparticles, and c) Fe_3O_4 -capped magnet-MSNs.

relative to that of linker-MSN and could also be attributed to the covalent-bond-induced pore-filling effect between the Fe_3O_4 nanoparticles and the mesoporous silica matrix. The high-angle powder XRD patterns of magnet-MSNs matched exactly that of the APTS- Fe_3O_4 nanoparticles (Figure 3b) and confirmed the presence of APTS- Fe_3O_4 on the surface of the linker-MSNs. The pore-filling effect was also confirmed by the N_2 adsorption/desorption isotherms of the Fe_3O_4 -capped magnet-MSNs. In contrast to the high surface area ($1018.0 \text{ m}^2 \text{ g}^{-1}$) of linker-MSNs, magnet-MSNs showed a

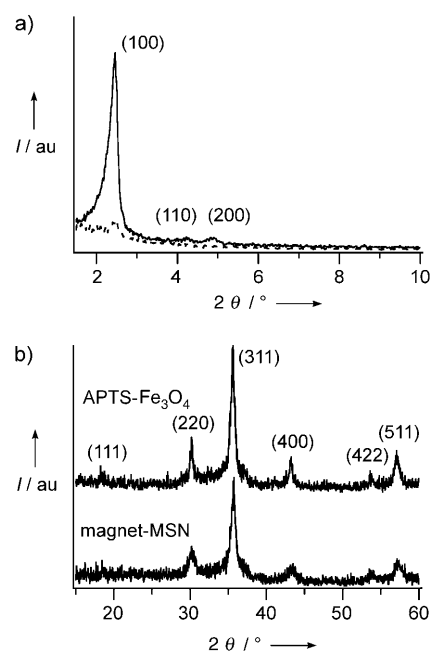


Figure 3. a) Low-angle X-ray diffraction (XRD) patterns of linker-MSN (—) and magnet-MSN (----) powders. b) High-angle XRD patterns of APTS-coated Fe_3O_4 nanoparticles (top) and magnet-MSN (below).

type I BET isotherm typical of nonporous materials, with a surface area of $296.0 \text{ m}^2 \text{ g}^{-1}$.^[42] The results indicated that most of the pore openings of the linker-MSN precursor were

indeed blocked by Fe_3O_4 nanoparticles. TEM investigations of magnet-MSN also provided direct evidence of the distribution of Fe_3O_4 nanoparticles on the organically functionalized linker-MSN material. The Fe_3O_4 nanoparticles are clearly visible as dark areas on the outside edge of the mesopores (Figure 2c). In contrast to the features observed for Fe_3O_4 -capped MSNs, the TEM micrograph of the linker-MSNs (Figure 2a) prior to capping with Fe_3O_4 nanoparticles showed smooth edges and a good contrast between the mesoporous channels and the silica matrix.

As mentioned earlier, the disulfide bonds between the MSNs and the Fe_3O_4 nanoparticles in the magnet-MSNs are labile and can be cleaved with disulfide reducing agents to release the trapped guest molecules from the mesopores. As the entire Fe_3O_4 -capped MSN carrier system is magnetic, the system can be magnetically directed to a site of interest from where the release can take place. To demonstrate the release of a drug with the magnet-MSNs under a magnetic field, two cuvettes were charged with fluorescein-loaded magnet-MSNs (50.0 mg each) dispersed in 3.00 mL of PBS solution (100.0 mM, pH 7.4). Both cuvettes were held against the tips of two magnets (magnetic stirrer-bar retrievers). As illustrated in Figure 4a, the magnet-MSNs were attracted to the walls of the cuvettes closest to the tips of the external magnets. Dithiothreitol (DTT, 48.5 mg, 3.15×10^{-4} mol) was added to one of the two cuvettes (left) for the release experiment, while the other cuvette (right) served as a control. After 2 days (Figure 4b), green fluorescence was clearly observed in the solution to which DTT was added

whereas no fluorescence could be observed from the control solution. As fluorescein-loaded magnet-MSNs do not fluoresce— Fe_3O_4 nanoparticles quench the fluorescence of fluorescein, as recently described^[47]—the result indicates that fluorescein molecules were indeed released from the magnet-MSNs by the introduction of the disulfide-reducing trigger DTT. Note, the color of the accumulated magnet-MSNs near the external magnet changed from black to gray after 4 days following the addition of DTT (Figure 4c). A white precipitate of MSNs was also observed at the bottom of the cuvette. As the black Fe_3O_4 nanoparticles are attracted to the external magnetic field whereas the MSNs are not, it is plausible that the Fe_3O_4 nanoparticle caps from the Fe_3O_4 -MSN ensembles were pulled in toward the magnet while the MSNs diffused away from the magnetic field as the disulfide linkage was cleaved by DTT.

Magnet-MSNs exhibited less than 1.0% release of fluorescein in PBS solutions (100.0 mM, pH 7.4) over a period of 132 h in the absence of trigger molecules (Figure 4d). This result suggested a good efficiency of the Fe_3O_4 nanoparticles to retain fluorescein molecules and prevent undesired leaching by capping the mesopores. Addition of 0.1 mM of disulfide reducing agents such as DHLA and DTT to a suspension of magnet-MSNs (13.0 mg) in PBS solution (3.00 mL, 100.0 mM, pH 7.4) triggered a rapid release of the mesopore-entrapped fluorescein. Within 48 h, 85% of the total release of fluorescein (40% of total loading) was attained; the maximum extent of release was achieved after 5 days (Figure 4d). With lipolic acid DHLA, the maximum percentage of

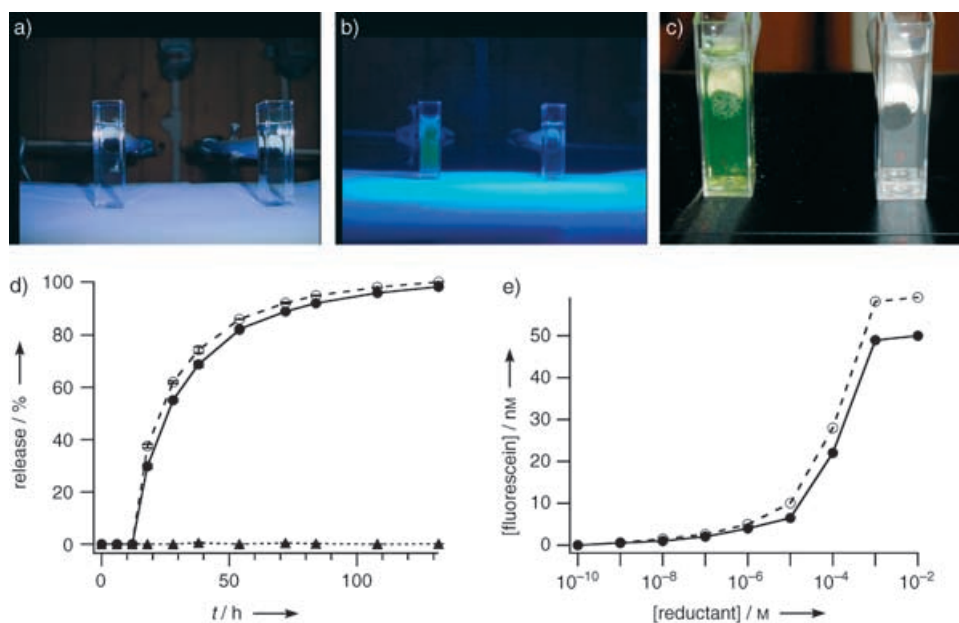


Figure 4. Photographs of two cuvettes charged with fluorescein-loaded magnet-MSNs (50.0 mg each) dispersed in 3.00 mL of PBS solution (100.0 mM, pH 7.4): a) Accumulation of magnet-MSNs on the walls of the cuvettes closest to the tips of the external magnets (magnetic stirrer-bar retrievers shown behind the cuvettes); b) 2 days after the addition of DTT (48.5 mg) to the solution contained in the cuvette on the left, green fluorescence was observed from the sample which signalled the release of encapsulated fluorescein from the matrix; c) 4 days after the addition of DTT, the color of the accumulated magnet-MSNs changed from black to gray. d) Controlled release of fluorescein from magnet-MSNs (13.0 mg) in 3.00 mL of PBS solution (100.0 mM, pH 7.4) triggered by 0.1 mM DHLA (●) or DTT (○). No noticeable release was observed in the absence of a reductant (▲). e) The dependence of the release of fluorescein from magnet-MSNs on the concentration of the reductant, measured 72 h after the addition of DHLA (●) or DTT (○).

fluorescein released was 31.4% of the total loading. Interestingly, the rates of release of fluorescein by the two different triggers showed similar diffusional kinetic profiles which indicates that the reducing powers of DHLA and DTT are similar. The similarity could be attributed to the fact that DHLA self-oxidizes into a disulfanyl-linked five-membered ring upon reducing the targeted disulfide bond, whereas DTT self-oxidizes into a disulfanyl-linked six-membered ring. The thermodynamic considerations of cyclizations into five- and six-membered rings should be similar. Furthermore, the amount of fluorescein released after 72 h following the addition of DHLA and DTT showed similar dependencies on the concentration of the trigger (Figure 4e) which indicates that the rate of release was dictated by the rate at which the Fe_3O_4 nanoparticle caps were removed.

To investigate the endocytosis and biocompatibility of our system, HeLa (human cervical cancer) cells ($\approx 10^5 \text{ cells mL}^{-1}$) were incubated overnight with magnet-MSNs (0.2 mg mL^{-1}) to allow the endocytosis of magnet-MSNs.^[40] The cells that took up magnet-MSNs were magnetically separated from those that did not. The isolated cells were treated with 0.001% of 4',6-diamidino-2-phenylindole (DAPI) dye in PBS solution (100.0 mM, pH 7.4) and placed in a cuvette. DAPI is known to form blue-fluorescent complexes with natural double-stranded DNA and has been widely used as a fluorescent dye for nucleus staining. These DAPI-stained, fluorescent cells were first accumulated to the right side wall of the cuvette by applying an external magnetic field—a commercially available grade N45 neodymium iron boron magnet. When the magnet was moved to the left side of the cuvette, the blue-fluorescent HeLa cells were clearly seen to move across the cuvette toward the magnet (Figure 5a–c)

indicating that the magnet-MSNs were indeed endocytosed by HeLa cells. To further confirm the endocytosis of magnet-MSNs, these HeLa cells were examined by confocal fluorescence microscopy. A series of fluorescence images of different cross-sections of magnet-MSN-containing HeLa cells were obtained by changing the focal depth every $1.2 \mu\text{m}$ vertically (see Supporting Information). Green fluorescence was clearly observed within the cell bodies of these HeLa cells upon excitation at 494 nm (Figure 5d) which strongly indicates that the mesopore-encapsulated fluorescein molecules were released inside the cells. As previously reported by Biaglow et al., cancer cell lines express significant amounts of DHLA.^[48] We believe that the efficient intracellular release of fluorescein was triggered by the high intracellular concentration of DHLA. To visualize the locations of the nuclei, the cells were excited at 358 nm (Figure 5e). The appearance of healthy intact nuclei and the visibility of fully grown cells by transmission (Figure 5f) suggested that the magnet-MSNs are biocompatible with HeLa cells in vitro under these experimental conditions.

In conclusion, we have demonstrated that mesoporous silica nanorods capped with superparamagnetic iron oxide nanoparticles—so-called magnet-MSNs—can be used as a stimuli-responsive controlled-release delivery carrier. Guest molecules that are smaller than 3 nm, such as fluorescein, could be encapsulated and released from the magnet-MSN delivery system by using cell-produced antioxidants (e.g. dihydrolipoic acid) as triggers in the presence of an external magnetic field. Furthermore, the biocompatibility and efficiency of intracellular delivery of the magnet-MSN system with human cervical cancer cells offer promising potential in utilization of this system to investigate various inter- and

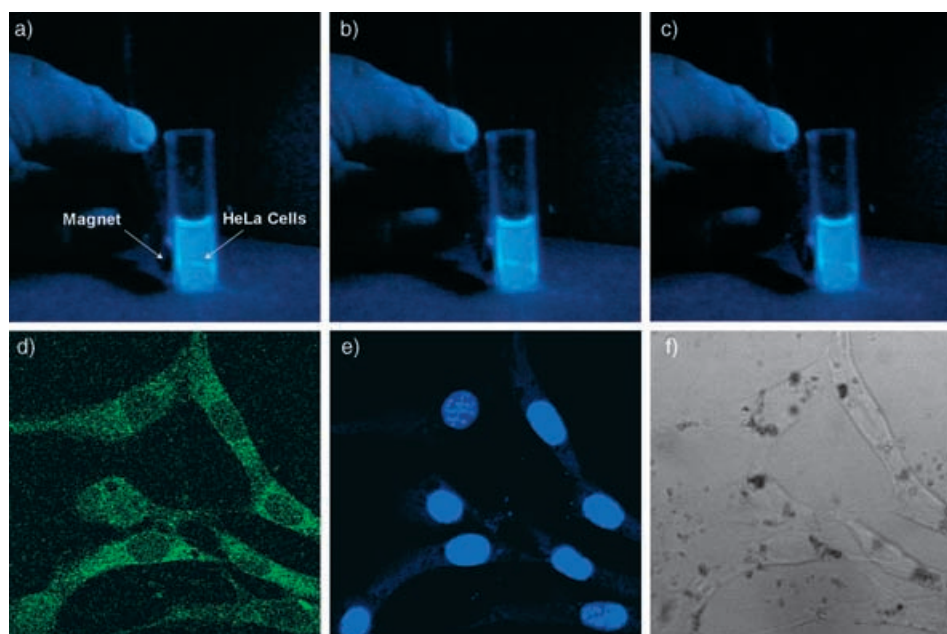


Figure 5. a–c) Single frames of photographs of HeLa cells with Fe_3O_4 -capped fluorescein-loaded MSNs traveling across the cuvette, propelled by magnetic force. d–f) Fluorescence confocal micrographs of HeLa cells after 10 h incubation with Fe_3O_4 -capped fluorescein-loaded MSNs: d) cells excited at 494 nm; e) cells excited in the UV region; f) a pseudo-brightfield image, where dark aggregations of magnet-MSNs can be clearly observed.

intracellular chemical/neurochemical communications in vitro. We envision that these magnet-MSNs could play a significant role in the development of new generations of site-selective controlled-release delivery devices and interactive sensory nanodevices.

Experimental Section

$\text{FeCl}_2 \cdot 4\text{H}_2\text{O}$, $\text{FeCl}_3 \cdot 6\text{H}_2\text{O}$, 3-aminopropyltriethoxysilane (APTS), 3-mercaptopropionic acid, 2-aldriethiol, 3-mercaptopropyltrimethoxysilane (MPTMS), tetraethylorthosilicate (TEOS), *n*-cetyltrimethylammonium bromide (CTAB), 1-(3-(dimethylamino)propyl)-3-ethylcarbodiimide hydrochloride (EDC), fluorescein, and dithiothreitol (DTT) were purchased from Aldrich and used as received. Dihydrolipoic acid (DHLA) was obtained from Sigma and used without further purification. Nanopure water (18.1 MHz) prepared from a Barnstead E-pure water-purification system was employed throughout. PBS (phosphate-buffered saline) solution (100.0 mM, pH 7.4) was used as the solvent for the loading experiments.

APTS-coated magnetite (Fe_3O_4) nanoparticles: Magnetic nanoparticles were prepared and coated with APTS according to a slightly modified reported procedure^[34] (see Supporting Information).

MCM-41-type mesoporous silica nanoparticles functionalized with 3-(propyldisulfanyl)propionic acid (linker-MSN): The thiol-MSN material was prepared according to a slightly modified version of our previously reported procedure^[31] (see Supporting Information). The purified thiol-MSNs (1.000 g) were treated with a solution of 2-carboxyethyl-2-pyridyl disulfide (1.340 g, 6.23×10^{-3} mol; prepared according to a reported procedure^[49]) in ethanol (80.00 mL) at room temperature for 24 h under vigorous stirring (vortex stirrer) to obtain the desired disulfide bond-exchange reaction. The resulting acid-functionalized MSN was filtered, washed with ethanol, and dried in air. The surface coverage of chemically accessible thiol groups was quantified at 7.01×10^{-4} mol g^{-1} .^[38]

Loading of fluorescein into the mesoporous framework of linker-MSN and the capping of the mesopores with APTS coated Fe_3O_4 nanoparticles: The purified linker-MSNs (80.0 mg) was stirred vigorously (vortex stirrer) in a solution of fluorescein (3.6×10^{-6} M) in PBS solution (8.00 mL, 100.0 mM, pH 7.4) for 24 h. Then, APTS-coated Fe_3O_4 nanoparticles (960.0 mg) were added to the suspension followed by 1-(3-(dimethylamino)propyl)-3-ethylcarbodiimide hydrochloride (EDC) (60.0 mg, 3.13×10^{-4} mol). The mixture was stirred vigorously (vortex stirrer) for another 48 h before the precipitate was filtered, washed extensively with buffer, and dried under vacuum. The precipitate (480.0 mg) was stirred vigorously again in PBS solution (10.00 mL, 100.0 mM, pH 7.4) for 48 h, followed by filtration and washing ($\times 7$) with PBS solution to remove physisorbed, uncapped fluorescein molecules from the exterior surface of the material. The purification procedure was repeated once more to further remove any physisorbed fluorescein, and the solid material was finally dried into a powder. All the washings were collected, and the loading of fluorescein (2.1×10^{-10} mol mg^{-1} linker-MSN) was calculated from the difference in the concentration of the initial solution of fluorescein and that of the reaction medium combined with the subsequent washings.

Endocytosis of Fe_3O_4 -capped MSNs in HeLa cells: Human cervical cancer (HeLa) cell lines were obtained from the American Tissue Culture Collection (ATCC) and were maintained using DMEM (Dulbecco's modified Eagle's medium) supplemented with horse serum (10%), L-glutamine (2.00 mM), penicillin (100 U mL^{-1}), streptomycin (100.0 mg mL^{-1}), and gentamicin (1.0 mg mL^{-1}). HeLa cells were seeded onto 6-well plates (1×10^5 cells in 3.00 mL of growth medium per well) 24 h prior to the experiment. After 24 h, the wells were seeded with Fe_3O_4 -capped MSNs (0.2 mg mL^{-1}) in growth medium. After 10 h, the medium was removed and the cells were washed with fresh growth medium. Then, the cells were trypsinized

with 0.25% trypsin. A magnet was used to keep the cells associated with the magnetic nanoparticles stationary while the remaining (nonmagnetic) cells were removed. The cells that took up the Fe_3O_4 -capped MSNs were centrifuged and resuspended in a solution of 4',6'-diamidino-2-phenylindole (DAPI, 100.0 $\mu\text{g mL}^{-1}$) in PBS (100.0 mM, pH 7.4).

Received: May 26, 2005

Published online: July 22, 2005

Keywords: drug delivery · fluorescence · magnetic properties · mesoporous materials · nanostructures

- [1] A. K. Gupta, A. S. G. Curtis, *J. Mater. Sci. Mater. Med.* **2004**, *15*, 493.
- [2] T. Neuberger, B. Schoepf, H. Hofmann, M. Hofmann, B. von Rechenberg, *J. Magn. Magn. Mater.* **2005**, *293*, 483.
- [3] A. S. Lubbe, C. Bergemann, J. Brock, D. G. McClure, *J. Magn. Magn. Mater.* **1999**, *194*, 149.
- [4] U. Schillinger, T. Brill, C. Rudolph, S. Huth, S. Gersting, F. Kroetz, J. Hirschberger, C. Bergemann, C. Plank, *J. Magn. Magn. Mater.* **2005**, *293*, 501.
- [5] F. Scherer, M. Anton, U. Schillinger, J. Henke, C. Bergemann, A. Kruger, B. Gansbacher, C. Plank, *Gene Ther.* **2002**, *9*, 102.
- [6] J. M. Perez, L. Josephson, T. O'Loughlin, D. Hoegemann, R. Weissleder, *Nat. Biotechnol.* **2002**, *20*, 816.
- [7] J. M. Perez, T. O'Loughlin, F. J. Simeone, R. Weissleder, L. Josephson, *J. Am. Chem. Soc.* **2002**, *124*, 2856.
- [8] J. W. M. Bulte, T. Douglas, B. Witwer, S.-C. Zhang, E. Strable, B. K. Lewis, H. Zywicki, B. Miller, P. van Gelderen, B. M. Moskowitz, L. D. Duncan, J. A. Frank, *Nat. Biotechnol.* **2001**, *19*, 1141.
- [9] J. Gellissen, C. Axmann, A. Prescher, K. Bohndorf, K. P. Lodemann, *Magn. Reson. Imaging* **1999**, *17*, 557.
- [10] P. S. Doyle, J. Bibette, A. Bancaud, J.-L. Viovy, *Science* **2002**, *295*, 2237.
- [11] D. Wang, J. He, N. Rosenzweig, Z. Rosenzweig, *Nano Lett.* **2004**, *4*, 409.
- [12] C. Xu, K. Xu, H. Gu, R. Zheng, H. Liu, X. Zhang, Z. Guo, B. Xu, *J. Am. Chem. Soc.* **2004**, *126*, 9938.
- [13] H. Gu, P.-L. Ho, K. W. T. Tsang, L. Wang, B. Xu, *J. Am. Chem. Soc.* **2003**, *125*, 15702.
- [14] A. K. Gupta, M. Gupta, *Biomaterials* **2005**, *26*, 3995.
- [15] A. Jordan, R. Scholz, P. Wust, H. Schirra, T. Schiestel, H. Schmidt, R. Felix, *J. Magn. Magn. Mater.* **1999**, *194*, 185.
- [16] I. Hilger, W. Andra, R. Herget, R. Hiergeist, H. Schubert, W. A. Kaiser, *Radiology* **2001**, *218*, 570.
- [17] D. C. F. Chan, D. B. Kirpotin, P. A. Bunn, Jr., *J. Magn. Magn. Mater.* **1993**, *122*, 374.
- [18] L. R. Hirsch, R. J. Stafford, J. A. Bankson, S. R. Sershen, B. Rivera, R. E. Price, J. D. Hazle, N. J. Halas, J. L. West, *Proc. Natl. Acad. Sci. USA* **2003**, *100*, 13549.
- [19] T.-J. Yoon, J. S. Kim, B. G. Kim, K. N. Yu, M.-H. Cho, J.-K. Lee, *Angew. Chem.* **2005**, *117*, 1092; *Angew. Chem. Int. Ed.* **2005**, *44*, 1068.
- [20] P. Chattopadhyay, R. B. Gupta, *Ind. Eng. Chem. Res.* **2002**, *41*, 6049.
- [21] J. F. Diaz, K. J. Balkus, Jr., *J. Mol. Catal. B* **1996**, *2*, 115.
- [22] Y.-J. Han, G. D. Stucky, A. Butler, *J. Am. Chem. Soc.* **1999**, *121*, 9897.
- [23] H. Takahashi, B. Li, T. Sasaki, C. Miyazaki, T. Kajino, S. Inagaki, *Microporous Mesoporous Mater.* **2001**, *44–45*, 755.
- [24] M. Vallet-Regi, A. Ramila, R. P. del Real, J. Perez-Pariente, *Chem. Mater.* **2001**, *13*, 308.
- [25] B. Munoz, A. Ramila, J. Perez-Pariente, I. Diaz, M. Vallet-Regi, *Chem. Mater.* **2003**, *15*, 500.

- [26] A. Ramila, B. Munoz, J. Perez-Pariente, M. Vallet-Regi, *J. Sol-Gel Sci. Technol.* **2003**, 26, 1199.
- [27] C. Tourne-Peteilh, D. Brunel, S. Begu, B. Chiche, F. Fajula, D. A. Lerner, J.-M. Devoisselle, *New J. Chem.* **2003**, 27, 1415.
- [28] M. Vallet-Regi, J. C. Doadrio, A. L. Doadrio, I. Izquierdo-Barba, J. Perez-Pariente, *Solid State Ionics* **2004**, 172, 435.
- [29] N. K. Mal, M. Fujiwara, Y. Tanaka, *Nature* **2003**, 421, 350.
- [30] R. Hernandez, H.-R. Tseng, J. W. Wong, J. F. Stoddart, J. I. Zink, *J. Am. Chem. Soc.* **2004**, 126, 3370.
- [31] C.-Y. Lai, B. G. Trewyn, D. M. Jeftinija, K. Jeftinija, S. Xu, S. Jeftinija, V. S. Y. Lin, *J. Am. Chem. Soc.* **2003**, 125, 4451.
- [32] J. A. Gruenhagen, C.-Y. Lai, D. R. Radu, V. S. Y. Lin, E. S. Yeung, *Appl. Spectrosc.* **2005**, 59, 424.
- [33] D. R. Radu, C.-Y. Lai, W. Wiench Jerzy, M. Pruski, V. S. Y. Lin, *J. Am. Chem. Soc.* **2004**, 126, 1640.
- [34] W. C. W. Chan, S. Nie, *Science* **1998**, 281, 2016.
- [35] M. Ma, Y. Zhang, W. Yu, H.-Y. Shen, H.-Q. Zhang, N. Gu, *Colloids Surf. A* **2003**, 212, 219.
- [36] S. Huh, W. Wiench Jerzy, B. G. Trewyn, S. Song, M. Pruski, V. S. Y. Lin, *Chem. Commun.* **2003**, 2364.
- [37] S. Huh, J. W. Wiench, J.-C. Yoo, M. Pruski, V. S. Y. Lin, *Chem. Mater.* **2003**, 15, 4247.
- [38] V. S. Y. Lin, C.-Y. Lai, J. Huang, S.-A. Song, S. Xu, *J. Am. Chem. Soc.* **2001**, 123, 11510.
- [39] D. R. Radu, C.-Y. Lai, J. Huang, X. Shu, V. S. Y. Lin, *Chem. Commun.* **2005**, 1264.
- [40] D. R. Radu, C.-Y. Lai, K. Jeftinija, E. W. Rowe, S. Jeftinija, V. S. Y. Lin, *J. Am. Chem. Soc.* **2004**, 126, 13216.
- [41] B. G. Trewyn, C. M. Whitman, V. S. Y. Lin, *Nano Lett.* **2004**, 4, 2139.
- [42] See Supporting Information for details.
- [43] B. Marler, U. Oberhagemann, S. Vortmann, H. Gies, *Micro-porous Mater.* **1996**, 6, 375.
- [44] H. Winkler, A. Birkner, V. Hagen, I. Wolf, R. Schmechel, H. Von Seggern, R. A. Fischer, *Adv. Mater.* **1999**, 11, 1444.
- [45] W.-H. Zhang, J.-L. Shi, L.-Z. Wang, D.-S. Yan, *Chem. Mater.* **2000**, 12, 1408.
- [46] W.-H. Zhang, J.-L. Shi, H.-R. Chen, Z.-L. Hua, D.-S. Yan, *Chem. Mater.* **2001**, 13, 648.
- [47] L. Josephson, M. F. Kircher, U. Mahmood, Y. Tang, R. Weisleder, *Bioconjugate Chem.* **2002**, 13, 554.
- [48] J. E. Biaglow, J. Donahue, S. Tuttle, K. Held, C. Chrestensen, J. Mieyal, *Anal. Biochem.* **2000**, 281, 77.
- [49] J. Carlsson, H. Drevin, R. Axen, *Biochem. J.* **1978**, 173, 723.